Solar Energy Materials & Solar Cells 119 (2013) 214–218

Contents lists available at ScienceDirect

Solar Energy Materials & Solar Cells

journal homepage: www.elsevier.com/locate/solmat

Development of thin-film solar cells using solar spectrum splitting technique

Sinae Kim [a,*], Shunsuke Kasashima [a], Porponth Sichanugrist [a], Taizo Kobayashi [c], Tokio Nakada [c], Makoto Konagai [a,b]

[a] Department of Physical Electronics, Tokyo Institute of Technology, Japan
[b] Photovoltaic Research Center (PVREC), Tokyo Institute of Technology, 2-12-1-NE-15, O-okayama, Meguro-ku, Tokyo 152-8552, Japan
[c] Department of Electrical Engineering and Electronics, Aoyama Gakuin University, 5-10-1 Fuchinobe, Sagamihara, Kanagawa 252-5258, Japan

ARTICLE INFO

Available online 29 August 2013

Keywords:
Spectrum splitting
Thin-film solar cell

ABSTRACT

To increase the performance of thin-film solar cells, the solar spectrum splitting technique has been considered and studied. It was found from simulations that the total efficiency of nearly 25% can be obtained at the splitting wavelength of 600 nm with the top cell using higher band gap material. Experiments have been carried out to verify the simulation results. Up to now the total efficiency of about 22.0% has been obtained using a-Si:H and $Cu(In_{1-x},Ga_x)Se_2$ as the top and bottom cells, respectively, at the splitting wavelength of 614 nm which is similar to the simulation results. This result shows that our developed splitting technique is promising for high-performance thin-film solar cells.

1. Introduction

Thin-film solar cells have been probed through many recent years due to their virtue of low production cost, large-scale deposition, low temperature production and high conversion efficiency. The thin film solar cell has come up with multi-junction solar cell structure because this structure utilizes the solar spectrum effectively. In general, the incident photon energy is much higher than the absorber's band gap energy, and the difference between two energies is released as heat losses. In the case of multi-junction solar cells, each component subcell absorbs photons whose energy corresponds to the band gap of each absorber. Then the thermal energy losses can be considerably suppressed with increasing numbers of junctions of solar cells. There have been many studies about various kinds of multi-junction structures and very-high efficiencies of even over 40% have been achieved with III–V compound semiconductor materials [1–7].

In order to realize the prerequisites, the spectrum splitting technique has been considered. The incident light is separated into some parts of spectral ranges by using optical splitters and each part is directed to individual component cells whose band gap energies correspond to that range. Various kinds of splitting techniques have been proposed and discussed in the literature [8] and they include dichroic filter with dielectric multilayer, luminescence solar concentrator with fluorescent dye, prism refraction, and holographic filter. The first demonstration of this spectrum splitting system at PV module level was presented by Borden et al. [9,10]. However expensive crystalline AlGaAs and Si have been used.

Furthermore, a research with the same approach using low cost dichroic mirror has been carried out [11]. GaInP and pc-Si type cells have been used, but again all of them are crystalline type solar cells whose manufacturing cost is considered to be high.

In this work, we have carried out a study to apply the splitting techniques to thin-film type solar cells such as amorphous silicon (a-Si) and $Cu(In_{1-x},Ga_x)Se_2$ (CIGS) since their manufacturing costs are lower. Besides that, a low cost dichroic mirror has also been developed; a-Si has been chosen since its band gap is more than 1.7 eV and can be changed by varying the deposition temperature and hydrogen dilution ratio. On the other hand, CIGS has been used in the bottom cell since its band gap can be minimized to as low as 1.0 eV.

Our spectrum splitting system was designed as shown in Fig. 1. First, the optical filter has been located at 45°, and a-Si top and CIGS bottom cells are placed to absorb the light at short and long wavelength regions, respectively. In this study we first theoretically calculated its performance and then the cells have been fabricated and measured.

2. Simulation model

To determine material parameter sets for both top and bottom cells, a numerical analysis was carried out using a one-dimensional device simulation program AMPS-1D (Analysis of Microelectronic and Photonic Structures) [12]. In order to make the best match to

* Corresponding author. Tel.: +81 0357342662.
E-mail address: kim.s.ap@m.titech.ac.jp (S. Kim).

0927-0248/$ - see front matter © 2013 Elsevier B.V. All rights reserved.
http://dx.doi.org/10.1016/j.solmat.2013.07.011

the spectral response of the top and bottom solar cells, four different splitting wavelengths (l_{SP}) (500, 600, 700 and 800 nm) have been used. Then for the top cell, band gap and thickness have been varied from 1.5 eV to 2.0 eV and 300 to 500 nm, respectively. On the other hand, the band gap of the bottom cell has been changed from 1.0 eV to 1.4 eV and its thickness has been fixed at 2000 nm. The electrical and optical parameters taken from experimental results and some literatures [13–19] for each layer are listed in Table 1.

3. Experiment details

The a-Si:H solar cells with i-layers having band gap of 1.85 eV have been fabricated by 60 MHz VHF-PECVD on the conventional ZnO:B coated glass with solar cell area of 0.086 cm^2. The cell structure is glass/ZnO:B/p-a-SiO:H/buffer/i-a-Si:H (1.85 eV, 300 nm)/n-μc-SiO:H/Ag/Al. In order to get wider band gap for a-Si:H solar cell, low temperature and high H_2 dilution have been employed while substrate temperature, inter-electrode distance, VHF power density and chamber pressure were kept constant at 150 °C, 2 cm, 1 mW/cm^2 and 50 Pa, respectively.

The structure of CIGS bottom cells was Al grid/ZnO:B/ZnO/CdS/CIGS/Mo/soda–lime glass. CIGS absorber layer was fabricated by a three-stage method using a molecular beam epitaxy (MBE) apparatus, which was equipped with elemental Cu, In, Ga, and Se Knudsen cells. The growth temperature at the first stage was about 300 °C, and those at the second and third stages were about 530 °C. The CdS buffer layer was deposited by a chemical bath deposition process and the non-doped ZnO/ZnO:B window layers were prepared by the MOCVD method. In this study, CIGS solar cell performance was evaluated by active area. The photo *J–V* characteristics of solar cells were measured under standard 1-sun illumination (AM1.5 100 mW/cm^2).

Optical filters with different splitting wavelengths 600 nm (model: 03LWP610), 650 nm (03LWP612), 700 nm (03LWP614), 750 nm (03LWP616) and 800 nm (03LWP618) which were commercially sold by CVI Melles Griot Corp. were used. Furthermore an optimized optical filter at splitting wavelength 614 nm developed by KANEKA Corp. was used in order to achieve higher performance.

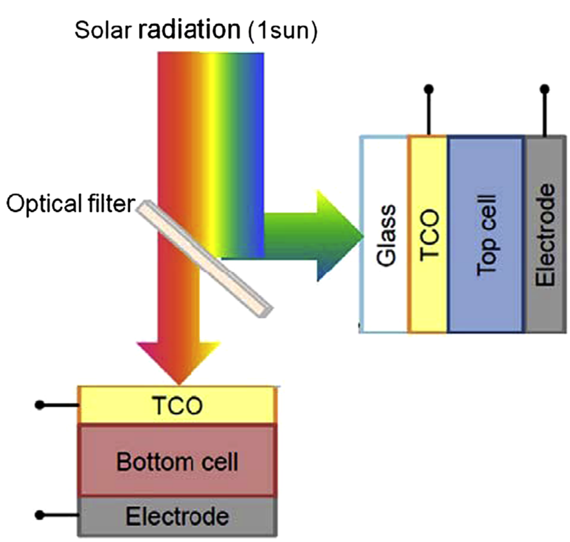

Fig. 1. Schematic diagram of four terminals photovoltaic device using the spectrum splitting technique.

4. Results and discussion

4.1. Simulation results

Fig. 2 shows the solar cell performances achieved from the simulation for top and bottom cells under various parameters. As can be expected, the efficiency of top cell decreases with shorter splitter wavelength while the one for bottom cell increases. This comes from the fact that less and more light are illuminated to the top and bottom cell respectively. Furthermore, the top cell with wider band gap has higher performance at shorter splitting wavelength due to its higher V_{oc}. Fig. 3 summarizes the total efficiency under different ranges of splitting wavelength. The total efficiency for the combination of the top cell with wider band gap

Table 1
Material parameters used in the simulation model.

(1) Top cell parameters				
Parameters and unit	p-a-SiC:H	i-a-Si:H	n-a-Si:H	
Thickness (nm)	10	300–500	10	
Optical gap E_g (eV)	1.7–2.2	1.5–2.0	1.5–2.0	
Relative permittivity	11.9	11.9	11.9	
Electron affinity (eV)	3.9	4.0	4.0	
Electron mobility μ_e (cm^2/V s)	5×10^{15}	0	0	
Hole mobility μ_h (cm^2/V s)	0	0	1×10^{19}	
Doping concentration (cm^{-3})	1×10^{20}	1×10^{20}	1×10^{20}	
Effective density of states (cm^{-3})	1×10^{20}	1×10^{20}	1×10^{20}	
(2) Bottom cell parameters				
Parameters and unit	n-ZnO:B	i-ZnO	n-CdS	p-CIGS
Thickness (nm)	1000	90	50	2000
Optical gap E_g (eV)	3.3	3.3	2.4	1.0–1.4
Relative permittivity	9	9	10	13.6
Electron affinity (eV)	4.5	4.5	3.75	3.85–4.25
Electron mobility μ_e (cm^2/V s)	0	0	0	2.01×10^{16}
Hole mobility μ_h (cm^2/V s)	5.7×10^{18}	5×10^{16}	2.1×10^{18}	0
Doping concentration (cm^{-3})	2.22×10^{18}	2.22×10^{18}	2.22×10^{18}	2.22×10^{18}
Effective density of states (cm^{-3})	1.78×10^{19}	1.78×10^{19}	1.78×10^{19}	1.78×10^{19}